Biosensors and Bioelectronics 192 (2021) 113497

Contents lists available at ScienceDirect

Biosensors and Bioelectronics

journal homepage: www.elsevier.com/locate/bios

A rapid, ultrasensitive voltammetric biosensor for determining SARS-CoV-2 spike protein in real samples

Lokman Liv [a,*], Gizem Çoban [a], Nuri Nakiboğlu [b], Tanıl Kocagöz [c]

[a] Electrochemistry Laboratory, Chemistry Group, The Scientific and Technological Research Council of Turkey, National Metrology Institute, (TUBITAK UME), 41470, Gebze, Kocaeli, Turkey
[b] Department of Chemistry, Faculty of Arts and Sciences, Balıkesir University, 10145, Balıkesir, Turkey
[c] Department of Medical Microbiology and Medical Biotechnology, Acibadem University, 34752, Istanbul, Turkey

ARTICLE INFO

Keywords:
Electrochemical biosensor
Coronavirus
SARS-CoV-2 spike protein
Viral detection
COVID-19
Voltammetry

ABSTRACT

The ongoing coronavirus disease 2019 (COVID-19) pandemic continues to threaten public health systems all around the world. In controlling the viral outbreak, early diagnosis of COVID-19 is pivotal. This article describes a novel method of voltammetrically determining severe acute respiratory syndrome coronavirus 2 (SARS-CoV-2) spike protein with a newly designed sensor involving bovine serum albumin, SARS-CoV-2 spike antibody and a functionalised graphene oxide modified glassy carbon electrode (BSA/AB/*f*-GO/GCE) or screen-printed electrode (BSA/AB/*f*-GO/SPE). The oxidation reaction based on the antibody–antigen protein interaction was evaluated as a response to SARS-CoV-2 spike protein at -200 mV and 1430 mV with the BSA/AB/*f*-GO/SPE and BSA/AB/*f*-GO/GCE, respectively. The developed sensors, BSA/AB/*f*-GO/SPE and BSA/AB/*f*-GO/GCE, could detect 1 ag/mL of virus spike protein in synthetic, saliva and oropharyngeal swab samples in 5 min and 35 min, and both sensors demonstrated a dynamic response to the SARS-CoV-2 spike protein between 1 ag/mL and 10 fg/mL. Real-time polymerase chain reaction (RT-PCR), rapid antigen test and the proposed method were applied to saliva samples. When compared to RT-PCR, it was observed that the developed method had a 92.5% specificity and 93.3% sensitivity. Moreover, BSA/AB/*f*-GO/SPE sensor achieved 91.7% accuracy compared to 66.7% accuracy of rapid antigen test kit in positive samples. In view of these findings, the developed sensor provides great potential for the diagnosing of COVID-19 in real samples.

1. Introduction

Coronavirus infectious disease 2019 (COVID-19) which is caused by severe acute respiratory syndrome coronavirus 2 (SARS-CoV-2) is currently leading to one of the deadliest pandemics in history. Due to the rapid spread of the disease in human infection and the lack of sufficient vaccine for all countries or an ineffective drug makes the pandemic very hard to control (WHO, 2020a; WHO, 2020b). On 5 June 2020, the disease's basic reproduction number (R_0), meaning the number of people infected by one person, ranged between 2 and 4, while the case fatality ratio was approximately 7% (WHO, 2020c). The average value of 3.17 obtained from 24 studies with 32 different R_0 values coincides with this situation (Billah et al., 2020). As a result, by 9 April, more than 133 million cases of COVID-19 and more than 2.9 million deaths had been tallied by the World Health Organization (WHO, 2020d). Although SARS-CoV-2 shows high genetic similarity to SARS coronavirus (SARS-CoV) and Middle East respiratory syndrome coronavirus (MERS-CoV), its rate of infection is significantly higher than SARS-CoV's and MERS-CoV's (Seo et al., 2020). Controlling the spread of SARS-CoV-2 has been challenging because most individuals experience COVID-19 asymptomatically, which significantly complicates detecting cases of infection (Torrente-Rodríguez et al., 2020). In turn, because the prevalence of asymptomatic cases remains unknown, the total number of cases continues to be underestimated (Li et al., 2020; Park et al., 2020a). For now, studies have estimated that the percent of asymptomatic COVID-19 infections is approximately 40% (Oran and Topol, 2020).

Although methods of diagnosing viral diseases abound in the literature, the most commonly used methods are real-time polymerase chain reaction (RT-PCR) (Chan et al., 2020; Lan et al., 2020; Park et al., 2020b; Van Kasteren et al., 2020; Yang et al., 2020), lateral flow immunoassay (LFIA) (Andryukov, 2020; Huang et al., 2020; Zeng et al., 2020) and electrochemical biosensing (Fabiani et al., 2020; Seo et al., 2020;

* Corresponding author.
E-mail address: lokman.liv@tubitak.gov.tr (L. Liv).

https://doi.org/10.1016/j.bios.2021.113497
Received 8 January 2021; Received in revised form 4 July 2021; Accepted 8 July 2021
Available online 13 July 2021

Torrente-Rodríguez et al., 2020; Vadlamani et al., 2020; Zhao et al., 2020; Liv, 2021). With some standard protocols in circulation, RT-PCR is the primary method of diagnosing such diseases, despite being slow and expensive and requiring personnel trained to perform nasopharyngeal swab sampling (Z. Li et al., 2020; Seo et al., 2020; Torrente-Rodríguez et al., 2020). Worse still, RT-PCR has shown a false-negative ratio of up to 67% within 1 to 5 d and as low as 21% even 8 d after exposure (Kucirka et al., 2020). By comparison, LFIA is a simple qualitative technique for determining antibodies that entails dropping and running samples on a supporting material. However, antibody testing remains unreliable, because antibodies are not immediately produced in the body, and asymptomatic carriers and immune individuals show no differentiation (Gong et al., 2020). Furthermore, LFIA has demonstrated exceptionally low sensitivity (Andryukov, 2020; Huang et al., 2020; Zeng et al., 2020). Last, prominent electrochemical methods, deriving from antibody-based (Fabiani et al., 2020; Torrente-Rodríguez et al., 2020; Vadlamani et al., 2020) and antigen-based (Seo et al., 2020; Torrente-Rodríguez et al., 2020; Zhao et al., 2020) studies, antibody-based methods involve preparing electrodes during immunoassay, which can take up to 5 h and have limit of detection (LOD) values at the high magnitude of ng/mL (Fabiani et al., 2020; Vadlamani et al., 2020). Liv (2021) has recently shown a method with a 0.01 ag/mL of LOD for the SARS-CoV-2 spike antibody in synthetic, saliva and oropharyngeal swab samples, while this method is important in terms of monitoring the disease after infection rather than early diagnosis. Beyond that, preparing antigen sensitive sensors can require 7 to 29 h (Seo et al., 2020; Torrente-Rodríguez et al., 2020; Zhao et al., 2020). In the method with the best LOD (200 copies/mL in a clinical specimen, 3 aM artificial target in synthetic media) in real samples, the step of determining the SARS-CoV-2 antigen takes 3 h, and the method has the most time-consuming sensor preparation of all–a full 29 h (Zhao et al., 2020).

In view of those drawbacks, faster, cheaper, easier, more sensitive methods of detecting such a rapidly spreading fatal disease, are critically needed. In our study, we aimed to develop a newly designed, easy-to-prepare, more sensitive sensor for voltammetrically determining the SARS-CoV-2 spike antigen protein. To that and, we produced biosensing platforms involving bovine serum albumin (BSA) and functionalised with the SARS-COV-2 spike antibody (AB) and graphene oxide (*f*-GO) modified glassy carbon electrode (GCE)–altogether, BSA/AB/*f*-GO/GCE–or a screen-printed electrode (SPE)–that is, BSA/AB/*f*-GO/SPE–for the simple, quick, cost-effective, sensitive determination of SARS-CoV-2 spike protein in synthetic and real samples.

2. Material and methods

2.1. Chemicals and equipment

SARS-CoV-2 spike antibody (Chimeric MAb Cat: 40150-D00), SARS-CoV-2 (2019-nCoV) spike S1-his recombinant protein (HPLC-verified, Cat: 40591-V08H), MERS-CoV spike/S1 protein (S1 Subunit, aa 1-725, His Tag, Cat: 40069-V08B1) and Influenza A H1N1 Hemagglutinin/H0A protein (Cat: 11055-VNAB) were obtained from Sino Biological and *Streptococcus Pneumoniae* antigen, the native extract was purchased from Native Antigen Company. Graphene oxide (GO, Powder, Sigma-Aldrich 796034), N-(3-Dimethylaminopropyl)-N′-ethylcarbodiimide hydrochloride (EDC, ≥98, Sigma-Aldrich 03450), N-Hydroxysuccinimide (NHS, 98%, Sigma-Aldrich 130672), bovine serum albumin (BSA, ≥98, Sigma-Aldrich 05470), phosphate buffered saline (PBS, tablet, Sigma-Aldrich P4417, 0.01 M phosphate buffer, 0.0027 M potassium chloride and 0.137 M sodium chloride, pH 7.4, at 25 °C) and the other chemicals were used as analytical reagent grade.

Ultrapure water was procured from Milli-Q Direct 8 system. All the spike antibody and antigen solutions were stored in protein LoBind Eppendorf tubes. The other solutions were stored in high-density polyethylene falcon tubes.

Voltammetric measurements were carried out by Metrohm Autolab PGSTAT 128N potentiostat/galvanostat. Three electrode system consisting of SARS-CoV-2 spike antibody and graphene oxide modified glassy carbon electrode (BSA/AB/*f*-GO/GCE, BASi MF-2012 GCE as supporting surface) as a working electrode, platinum wire (BASi MW-1032, 7.5 cm) as a counter electrode and Ag/AgCl/3 M NaCl (BASi MF-2052 RE-5B) as a reference electrode for the macro detection system. Metrohm Dropsens screen-printed electrode (SPE, C11L) consisting of carbon ink working and counter electrodes, and Ag/AgCl reference electrode was used as a supporting surface for the micro detection system. Avec Av-203 table lamp stand and General Electric 250W infrared lamp (E27, 125 mm) were used to remove solvent and dry the graphene oxide suspension on the bare electrodes.

All simulated and clinical samples were analysed for the presence of SARS-CoV-2 using commercial PCR kits (Bioeksen, Istanbul, Turkey) according to the manufacturer's instructions using the RT-PCR instrument (Biorad CFX Connect Real-Time PCR system).

The absence and presence of SARS-CoV-2, in simulated and clinical samples, were also analysed by RapidFor SARS-CoV-2 Rapid Antigen Test–Colloidal Gold (Vitrosens, Istanbul, Turkey).

Mettler Toledo Seven Compact pH meter with InLab Expert Pro-ISM combined pH electrode was used for the preparation of buffer solutions.

ISOLAB 3 L ultrasonic bath was used for the related cleaning processes.

The stability measurements of the developed sensor, BSA/AB/f-GO/SPE, at 25 °C and 37 °C were performed by using NUVE ID 300 and Angelantoni/ACS Discovery DY340 climatic test chambers, respectively.

FEI Quanta FEG 250 environmental scanning electron microscope and FEI Quanta 250 XFLASH 5030 energy dispersive X-ray spectroscopy were used for the characterization of sensors developed.

2.2. Preparation of SARS-CoV-2 sensors

To prepare the BSA/AB/*f*-GO/GCE, the GCE surface was polished with 0.05 μm of aluminum oxide on felt and rinsed with ultrapure water, followed by exposure to ultrasonic waves in a 1:1 ethanol–ultrapure water mixture alternated with ultrapure water. After 3 μL of 20 mg/mL GO was deposited onto the GCE surface and dried under an infrared lamp at 85 °C, 5 μL of 200 mM of EDC and 200 mM of NHS were dropped onto the GO/GCE for 30 min at room temperature to functionalise the surface for the covalent immobilization of the SARS-CoV-2 spike antibody (Kailashiya et al., 2015). After being washed with 1X PBS solution, 10 μL of the 10 μg/mL SARS-CoV-2 spike antibody was dropped onto the functionalised GO/GCE (*f*-GO/GCE) surface and incubated for 1 h to obtain the AB/*f*-GO/GCE. Last, the sensor was gently rinsed with 1X PBS solution and blocked with 2% BSA (i.e. prepared in 1X PBS solution) for 10 min (Sanchez et al., 2007; Tran et al., 2012; Wang et al., 2013). The sensor denoted as BSA/AB/*f*-GO/GCE was stored at 4 °C until further measurement.

All steps for preparing the BSA/AB/*f*-GO/SPE were the same as for BSA/AB/*f*-GO/GCE, except polishing. The procedure of preparing the sensors is illustrated in Fig. 1.

2.3. Voltammetric measurement

Because the BSA/AB/*f*-GO/GCE was used in the solution medium, the SARS-CoV-2 spike protein was kept on the sensor for 30 min before being measured. On the BSA/AB/*f*-GO/SPE, by contrast, it was measured immediately. Square wave voltammetry (SWV) measurements were taken between -1.5 V and 2.3 V for the BSA/AB/*f*-GO/GCE and between -1.5 V and 1 V for the BSA/AB/*f*-GO/SPE. The peaks at -200 mV and 1430 mV were evaluated as a response to the SARS-CoV-2 spike protein for the BSA/AB/*f*-GO/SPE and the BSA/AB/*f*-GO/GCE, respectively. The SWV parameters of step potential, pulse amplitude and frequency were 5 mV, 20 mV and 10 Hz, also respectively. The solution consisting of 0.01 M of PBS solution at pH 7.5 as a supporting electrolyte

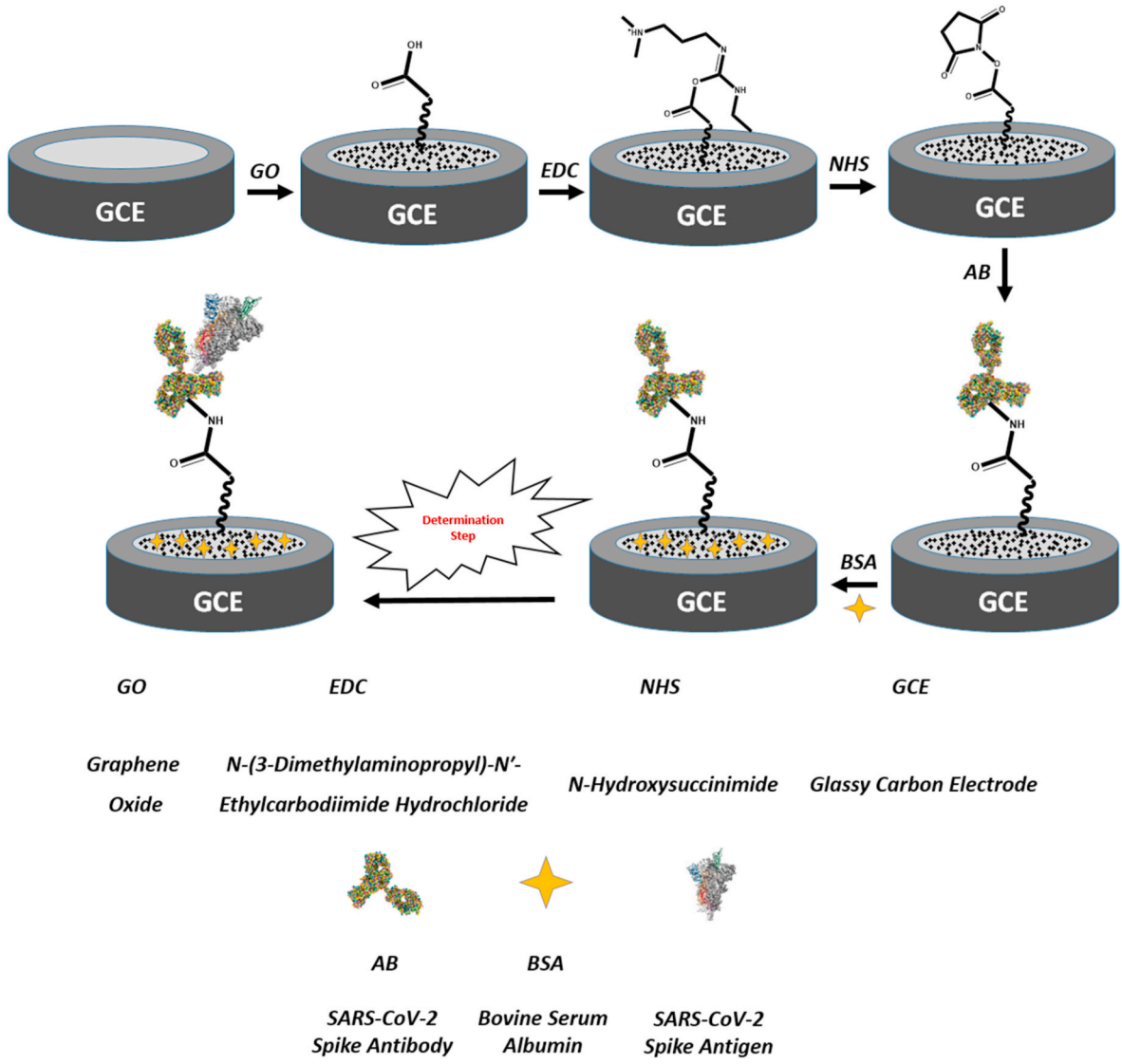

Fig. 1. Schematic presentation of the procedure of preparing the BSA/AB/*f*-GO/GCE.

and the proper amount of SARS-CoV-2 spike protein or real sample was used for both sensors. Measurements were recorded at 21 ± 3 °C and 45 ± 15% relative humidity.

2.4. Simulated and clinical samples

Gargle and mouthwash samples were obtained using drinking water with low ion concentration. Simulated samples were prepared by obtaining gargle and mouthwash fluid from volunteers and adding SARS-CoV-2 grown in cell culture and inactivated by gamma irradiation. Clinical samples were selected among gargle and mouthwash samples which were previously studied by RT-PCR for the presence of SARS-CoV-2. (Ethical approval for the study was obtained from Acibadem University Ethical Committee, ATADEK approval No: 2020-14/2.)

2.5. Sample preparation for voltammetric measurement

The prepared simulated and clinical gargle and mouthwash samples were pretreated with lysis buffer (i.e. 50 mM of Tris-Tris.HCl at pH 7.5, 100 mM of NaCl, 1 mM of dithiothreitol and 5% glycerol) to extract the protein residues. Afterward, 5 μL of the pretreated normal and SARS-CoV-2 spike antigen protein spiked-samples were analysed with BSA/AB/*f*-GO/GCE or BSA/AB/*f*-GO/SPE using external calibration by voltammetry.

3. Results and discussion

3.1. Sensor characterisation

Cyclic voltammetry (CV), electrochemical impedance spectroscopy (EIS), scanning electron microscopy (SEM) and energy dispersive X-ray spectroscopy (EDX) were used to confirm each modification of the working electrode. Cyclic voltammograms of the GCE, GO-modified GCE (GO/GCE), the EDC and NHS functionalised GO/GCE (*f*-GO/GCE), the SARS-CoV-2 spike antibody immobilised on the *f*-GO/GCE (AB/*f*-GO/GCE) and BSA modified AB/*f*-GO/GCE (BSA/AB/*f*-GO/GCE) in 1 mM of $K_3[Fe(CN)_6]$ and 1 mM of $K_4[Fe(CN)_6]$ appear in Fig. 2A. EIS spectra of the GO/GCE, AB/*f*-GO/GCE and BSA/AB/*f*-GO/GCE appear in Fig. 2B, while EIS spectra of the GCE and *f*-GO/GCE appear in Fig. S1 and Fig. S2, respectively. The lowest and highest peak currents belonging to the redox couple were obtained with the GCE and GO/GCE, also respectively. After the antibody and BSA were modified on the electrode's surface, the peak currents dropped due to the biosensor's diminishing effective surface area (Fig. 2A). As shown in Table S1, EIS with the $R_s(R_{ct}C_{dl})$ circuit yielded R_s (i.e. solution resistance—data not shown), R_{ct} (i.e. charge transfer resistance) and C_{dl} (i.e. double-layer

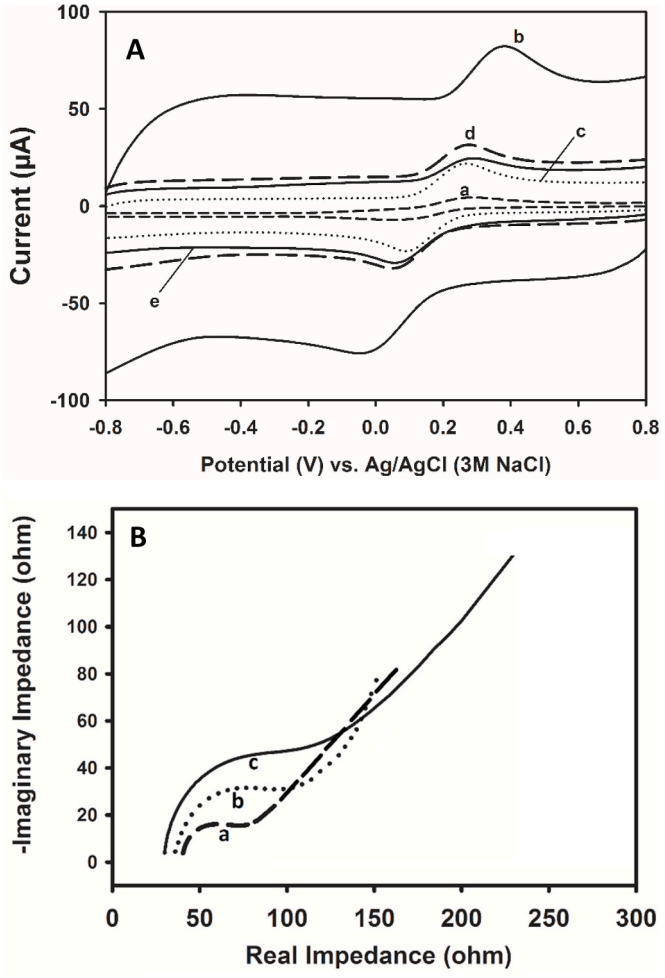

Fig. 2. A) Cyclic voltammograms of (a) GCE, (b) GO/GCE, (c) *f*-GO/GCE, (d) AB/*f*-GO/GCE and (e) BSA/AB/*f*-GO/GCE in 1 mM of $K_3[Fe(CN)_6]$ and 1 mM of $K_4[Fe(CN)_6]$ with a scan rate of 50 mV/s. B) EIS spectrum of (a) GO/GCE, (b) AB/*f*-GO/GCE and (c) BSA/AB/*f*-GO/GCE in 1 mM of $K_3[Fe(CN)_6]$, 1 mM of $K_4[Fe(CN)_6]$ and 0.1 M of KCl between 50,000 and 0.5 Hz.

capacitance) values indicating that the GO/GCE had the highest electron transfer rate and the GCE the lowest. Furthermore, when BSA was deposited onto the AB/*f*-GO/GCE, R_{ct} increased as active sites decreased. Such evidence confirms that the results of EIS aligned with the results of CV. SEM images and EDX spectra for the GO/GCE, *f*-GO/GCE, AB/*f*-GO/GCE and BSA/AB/*f*-GO/GCE, shown in Fig. 3, show that the electrodes' surface became more macro structured after the antibody and BSA were modified, owing to the large antibody and BSA molecules. Because the GO/GCE's porous structure allows adsorbing nitrogen in the air, nitrogen was expected in EDX analysis and also expected, the ratio of nitrogen to oxygen increased with the functionalisation of the GO/GCE's surface with EDC and NHS. It has been observed that the rate of nitrogen on the surface has decreased significantly after the AB modification on the *f*-GO/GCE since the binding of the antibody to the surface is generally carried out through nitrogen. Carbon, oxygen and nitrogen ratios changed at each modification, which confirms that the composition of the electrodes' surfaces ultimately changed.

3.2. Cyclic voltammetric characteristics of the system

CV was used to determine the electrode reaction mechanism belonging to the SARS-CoV-2 spike protein by using the BSA/AB/f-GO/GCE. As depicted in Fig. 4A, the sensor in 0.01 M of PBS solution (pH 7.5) has two oxidation and single reduction peaks belonging to the BSA/AB/*f*-GO/GCE at -200 mV (Fig. 4A inset), 1430 mV and -950 mV, respectively. The peak at -200 mV and 1430 mV proportionally increased with the addition of the SARS-CoV-2 spike protein into the solution, whereas the peak at -950 mV disproportionally increased. In the narrower potential range between 0.9 V and 2.3 V, however, the spike protein peak on the right was not observed in Fig. 4B; therefore, we concluded that the peak on the right was a product of the sequential oxidation reaction. Added to that, both peaks at -200 mV and 1430 mV increased with proportional amounts of the SARS-CoV-2 spike protein. Unlike the SARS-CoV-2 spike protein on the sensor surface in our previous study (Liv, 2021), the groups containing heteroatoms such as hydroxyl on the surface of the biosensor belonging to the SARS-CoV-2 spike antibody were oxidized during the anodic scan. The peak height of the biosensor increased in the presence of the SARS-CoV-2 spike protein in 0.01 M (pH 7.5) PBS solution due to the increasing oxidation ability belonging to the interaction between the SARS-CoV-2 spike antigen and antibody protein.

3.3. Optimisation studies

Because the concentration of antibody implicitly affects the performance of sensors, concentrations of 1.0, 2.5, 5.0, 10.0, 25.0 and 50.0 μg/mL of the SARS-CoV-2 spike antibodies (10 μL of each antibody solution) were separately incubated onto the functionalised GO/GCE surface. Ultimately, 10 μg/mL was chosen as optimal antibody concentration (Fig. S3A). Beyond that, the binding time of the antibody varied between 30 and 180 min, 60 min was used in further measurements (Fig. S3B). Last, the effects of pH and concentration of PBS solution were also investigated, with pH 7.5 and 0.01 mol/L (1X) specified as optimal values, as shown in Fig. S3C and Fig. S3D, respectively.

3.4. Method validation

The calibration voltammograms and plots representing the SARS-CoV-2 spike protein for both the BSA/AB/*f*-GO/GCE and BSA/AB/*f*-GO/SPE appear in Fig. 5. BSA/AB/*f*-GO/GCE and BSA/AB/*f*-GO/SPE sensors are able to detect 1 ag/mL of the SARS-CoV-2 spike protein in 1X PBS solution, saliva and oropharyngeal swab samples, respectively. Both sensors demonstrated a dynamic response to the SARS-CoV-2 spike protein between 1 ag/mL and 10 fg/mL (Fig. 5). The relative standard deviation values were 6.20%, 2.41% and 2.17% for BSA/AB/*f*-GO/GCE, and 4.85%, 3.63% and 2.35% for BSA/AB/*f*-GO/SPE at the concentration levels of 10 ag/mL, 100 ag/mL and 1000 ag/mL SARS-CoV-2 spike protein, respectively. Among the developed sensors, the BSA/AB/*f*-GO/SPE remarked in terms of cheapness, rapidity and sensor disposability, whereas the BSA/AB/*f*-GO/GCE drew attention in terms of ease of measurement and the clarity of voltammograms obtained.

Among other results, when the cross-reactivity effects of the spike proteins, MERS-CoV, pneumonia and influenza A, were examined, no significant change emerged in the baseline signal for the MERS-CoV and pneumonia spike protein, while it was + 5.4% for influenza A spike protein. Furthermore, the interference effects of disrupting the binding between the SARS-CoV-2 antibody and antigen protein were examined and no significant difference was observed in the signal of interaction between SARS-CoV-2 antibody and antigen protein as shown in Fig. S4. These results show that the developed biosensors do not show cross-reactivity or interaction-disrupting interference effects caused by MERS-CoV, pneumonia and influenza A spike proteins and that it selectively responds to the SARS-CoV-2 spike protein. Among the electrochemical methods in the literature, in addition to the cross-reactivity of the virus spike proteins mentioned above, there is no study in which the effects of these virus spike proteins on the binding between the SARS-CoV-2 spike protein and the antibody. Although the interfering spike proteins of these viruses do not bind to the surface of the sensor, their effects after the binding of SARS-CoV-2 spike protein are extremely important as they may affect positive and negative diagnostics.

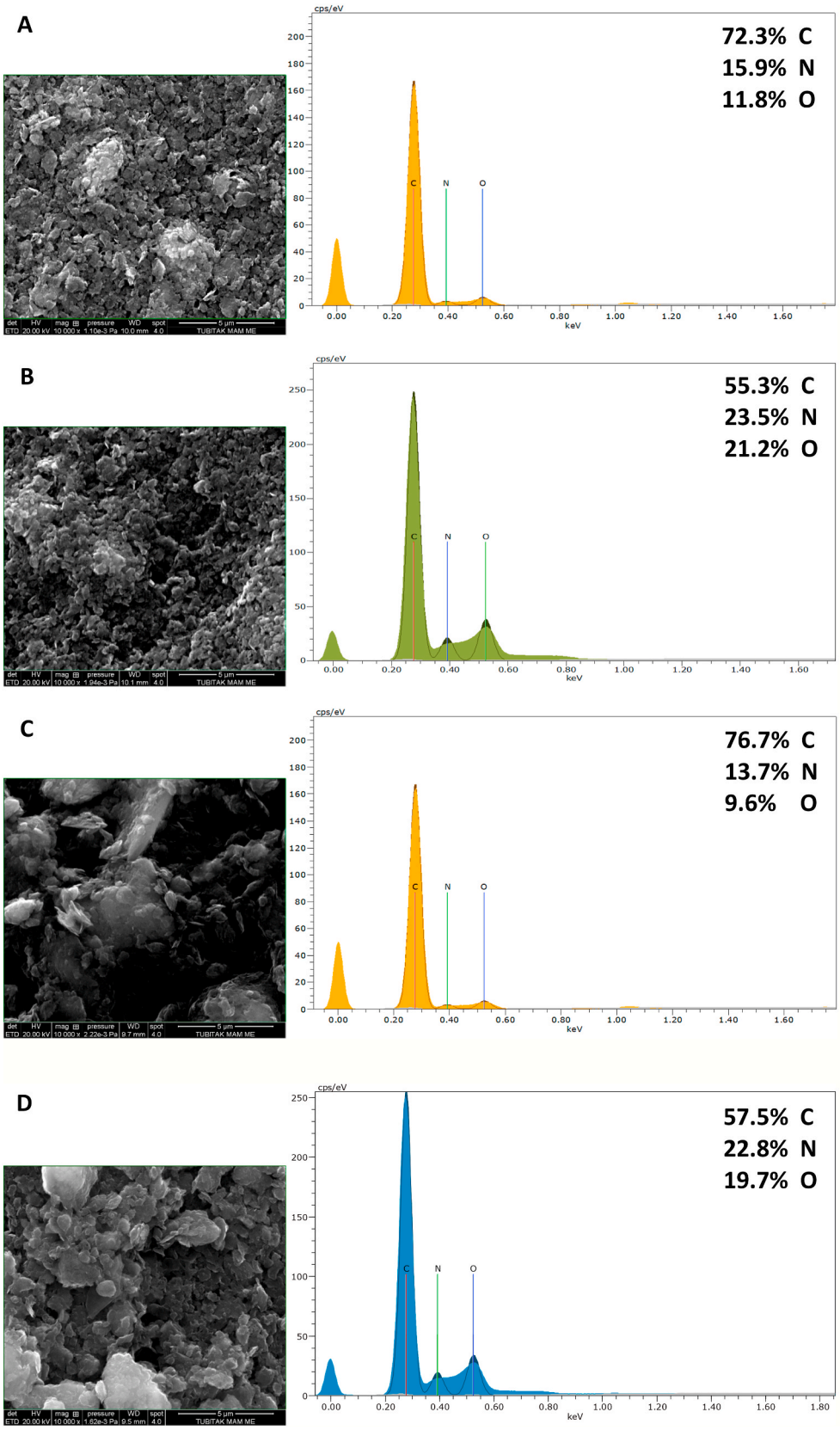

Fig. 3. SEM images and EDX spectra for A) GO/GCE, B) *f*-GO/GCE, C) AB/*f*-GO/GCE and D) BSA/AB/*f*-GO/GCE. SEM analysis: 20 kV voltage, 4.0–4.5 spot values, ETD detector. EDX analysis: SLEW/30 mm^2 detector, Energy resolutions; manganese: <127 eV FWHM at Mnkα, fluorine: 57 eV FWHM at Fkα and carbon: 51 eV FWHM at Ckα (atomic percentages were given in EDX spectra).

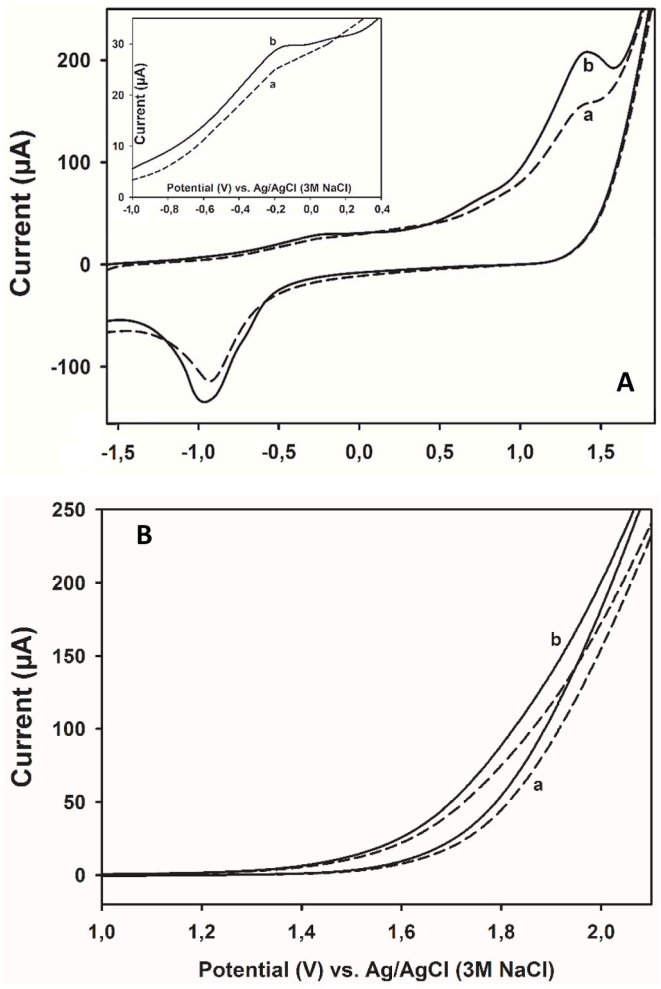

Fig. 4. Cyclic voltammograms obtained at A) wide potential range and B) narrow potential range using BSA/AB/*f*-GO/GCE sensor (a-dashed line) before and (b-solid line) after addition of 1 ng/L SARS-CoV-2 spike protein in 0.01 M pH 7.5 PBS solution with a scan rate of 50 mV/s.

3.5. Antigen protein and virus spiked sample analysis

The described method was applied to the SARS-CoV-2 spike protein spiked-saliva and oropharyngeal swab samples to voltammetrically determine the SARS-CoV-2 spike protein. The recovery and relative standard deviation values were between 99.82%–105.77% and 3.53%–5.97%, respectively. The voltammograms and results of the sample application are depicted in Fig. S5, Fig. S6 and Table S2, also respectively. The results suggest that the proposed method has good accuracy.

During the first week of COVID-19 symptoms, infected individuals have viruses in the range of 10^4 copy/mL to 10^8 copy/mL in saliva samples as well as in sputum and throat swab samples. In the second week, the amount of virion can decrease to 10^3 copy/mL levels, which indicates a minor change (Zhu et al., 2020). To that end, the simulated virus spiked-gargle and -mouthwash samples were used to observe the performance of the proposed method with several concentration levels from 1.25×10^3 to 1.25×10^5 copy/mL. The voltammograms show the peak height related to the concentration of the virus regarding the peak height of negative control using the BSA/AB/*f*-GO/SPE as seen in Fig. S7. The results showed that the developed method can be successfully used for 2 weeks after the onset of symptoms and early diagnosis of COVID-19.

3.6. Clinical sample analysis

Clinical samples were tested by using the described method, RT-PCR and rapid antigen test to appraise the efficiency of the disposable BSA/AB/*f*-GO/SPE sensor. To this end, the pretreated gargle and mouthwash samples were collected from healthy individuals and COVID-19 suspected patients, 80 negative and 30 positive samples identified by both RT-PCR and rapid antigen test were analysed with the proposed method. It was decided to set 450 nA (ΔI_p) current increase as threshold for positive samples, and 74/80 samples for negative results and 28/30 samples for positive results were in agreement with RT-PCR and rapid antigen test results that depict the 92.5% specificity and 93.3% sensitivity for negative and positive samples as seen in Table 1, respectively.

In addition, in order to compare the results of the rapid antigen test and BSA/AB/*f*-GO/SPE sensor, 12 different samples with positive RT-PCR results were randomly selected by TRaNS (Stratified Random Sample Selection) software and analysed with both the rapid antigen test and BSA/AB/*f*-GO/SPE sensor. As a result, it was observed that the BSA/AB/*f*-GO/SPE sensor achieved 91.7% accuracy compared to 66.7% accuracy of rapid antigen test kit in positive samples. It reflected the fact that the developed sensor responded more accurately than rapid antigen test, especially for positive samples. In this case, it is crucial to indicate that the sensor and method developed will significantly reduce the false-negative ratio compared to the rapid antigen test.

3.7. Sensor reusability

The reusability of BSA/AB/f-GO/GCE was examined in the presence of 10 ag/mL SARS-CoV-2 spike protein taking the criterion as ±5% change in peak height. The first measurement revealed that the sensor can be used twice more after being washed with 0.1 M of NaCl in 1X PBS solution (pH 7.5), meaning that one sensor can perform three measurements (Fig. S8). To the best of our knowledge, there is no such study about the reusability of electrochemical sensors in the literature. Considering that tens of millions of COVID-19 tests are carried out daily in the world, it is thought that the wash-reuse method will reduce the sensor cost by three times, which may lead to a financial breakthrough for COVID-19 testing.

3.8. Sensor stability

Sensor stability was examined by measuring the peak height at the end of each 7 d for 42 d. After the BSA/AB/*f*-GO/SPE sensors were prepared, they were stored in an argon atmosphere at 25 °C and 37 °C until measurement. The sensor had a diminishing signal trend, and when this trend was expressed with equations, $Relative\ signal(\%) = -0.1973\ Day + 99.583$ for 25 °C and $Relative\ signal(\%) = -0.2611\ Day + 98.508$ for 37 °C, as seen in Fig. S9, it was observed that the signal received on the first day was preserved as 91.5% and 88.1% at 25 °C and 37 °C on the 42nd day, respectively. As a result, the sensor is a very stable platform for diagnosing COVID-19 despite the strict temperature conditions. Monitoring the sensor performance for a long time and under different temperature conditions is of great importance for the commercialisation of the produced sensor and diagnosis at the bedside.

4. Conclusions

In this study, novel, cheap, selective and ultrasensitive biosensor platforms were developed for the rapid (<5 min) detection of SARS-CoV-2 spike protein in clinical samples. The results showed that the peak height increased with the interaction between the SARS-CoV-2 spike antigen and the antibody protein was not affected by the spike proteins of MERS-CoV, pneumonia and influenza A. Moreover, the cross-reactivity of these proteins with our produced biosensor platforms was not observed. The developed method exhibited excellent reliability and accuracy for the diagnosing of COVID-19 in real samples and a perfect

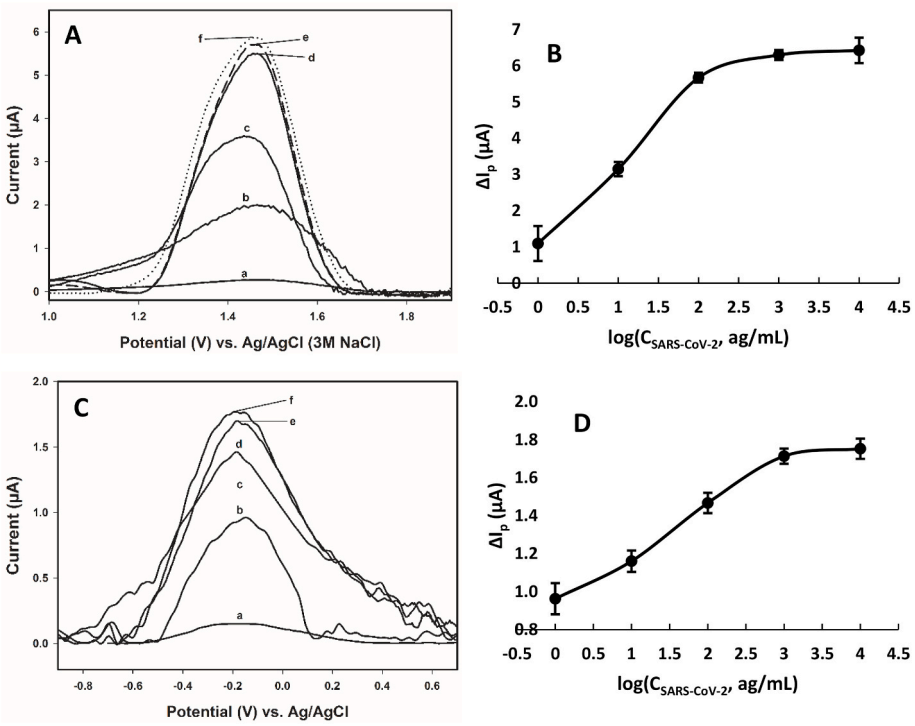

Fig. 5. The calibration voltammograms (A, C) and curves (B, D) at BSA/AB/*f*-GO/GCE (A, B) and BSA/AB/*f*-GO/SPE (C, D) in 0.01 M pH 7.5 PBS solution. Conditions: 10 μL 10 μg/mL SARS-CoV-2 antibody and 1h antibody immobilization time. (a) 0.01 M pH 7.5 PBS solution, (b) + 1 ag/mL, (c) + 10 ag/mL, (d) + 100 ag/mL, (e) + 1 fg/mL and (f) + 10 fg/mL SARS-CoV-2 spike protein.

Table 1
Comparison of results obtained from RT-PCR, rapid antigen test and BSA/AB/*f*-GO/SPE for COVID-19 positive gargle and mouthwash samples.

Sample	RT-PCR result	Rapid antigen test result	BSA/AB/*f*-GO/SPE result	Sample	RT-PCR result	Rapid antigen test result	BSA/AB/*f*-GO/SPE result
Patient#1	+	+	+	Patient#A	+	+	+
Patient#2	+	+	+	Patient#B	+	+	+
Patient#3	+	+	+	Patient#C	+	+	+
Patient#4	+	+	+	Patient#D	+	+	+
Patient#5	+	+	+	Patient#E	+	–	+
Patient#6	+	+	+	Patient#F	+	–	+
Patient#7	+	+	+	Patient#G	+	+	+
Patient#8	+	+	+	Patient#H	+	+	+
Patient#9	+	+	–	Patient#I	+	+	+
Patient#10	+	+	+	Patient#J	+	–	–
Patient#11	+	+	+	Patient#K	+	+	+
Patient#12	+	+	+	Patient#L	+	–	+
Patient#13	+	+	+				
Patient#14	+	+	+				
Patient#15	+	+	+				
Patient#16	+	+	+				
Patient#17	+	+	+				
Patient#18	+	+	+				
Patient#19	+	+	+				
Patient#20	+	+	+				
Patient#21	+	+	+				
Patient#22	+	+	+				
Patient#23	+	+	+				
Patient#24	+	+	–				
Patient#25	+	+	+				
Patient#26	+	+	+				
Patient#27	+	+	+				
Patient#28	+	+	+				
Patient#29	+	+	+				
Patient#30	+	+	+				

agreement with the RT-PCR results. Besides, it was obtained better results compared to the rapid antigen test.

It is crucial to state that the sensor can be used even a long time after preparation and one sensor can be used three times in positive samples, and hence it will minimize the testing cost. Moving forward, the BSA/AB/*f*-GO/SPE developed could be easily fabricated and provided as a ready-to-use kit on a commercial scale due to the prominent features such as low-cost, fast and highly sensitive and selective recognition of

the SARS-CoV-2 spike protein for the diagnosing of COVID-19 in real samples. In addition to these features, the GCE-based sensor is able to measure the SARS-CoV-2 spike protein at both -200 mV and 1430 mV and can be used many times with re-preparation. Last, since the method can be performed with portable voltammetric analyzers, it may provide an important potential of use for COVID-19 screening tests that can be performed by mobile healthcare teams.

CRediT authorship contribution statement

Lokman Liv: Conceptualization, Methodology, Validation, Formal analysis, Investigation, Writing – original draft, Writing - review & editing, Visualization, Supervision, Project administration. **Gizem Çoban:** Validation, Investigation. **Nuri Nakiboğlu:** Investigation, Writing – original draft, Writing - review & editing. **Tanıl Kocagöz:** Methodology, Resources, Investigation, Writing - review & editing.

Declaration of competing interest

The authors declare that they have no known competing financial interests or personal relationships that could have appeared to influence the work reported in this paper.

Acknowledgements

This study was performed in the Electrochemistry Laboratory of TUBITAK UME. The authors would like to thank to Melisa Yener, Şevval Arzu Can and Hilal Kayabay for performing some voltammetric measurements, and Sevgi Gülyüz at TUBITAK MAM-Materials Institute for SEM and EDX measurements.

Appendix A. Supplementary data

Supplementary data to this article can be found online at https://doi.org/10.1016/j.bios.2021.113497.

References

Andryukov, B.G., 2020. AIMS Microbiol. 6, 280–304.
Billah, A., Miah, M., Khan, N., 2020. PLoS One 15, e0242128.
Chan, J.F., Yip, C.C., To, K.K., Tang, T.H., Wong, S.C., Leung, K.H., Fung, A.Y., Ng, A.C., Zou, Z., Tsoi, H., Choi, G.K., Tam, A.R., et al., 2020. J. Clin. Microbiol. 58, e00310–e00320.
Fabiani, L., Saroglia, M., Galatà, G., De Santis, R., Fillo, S., Luca, V., Faggioni, G., D'Amore, N., Regalbuto, E., Salvatori, P., Terova, G., Moscone, D., et al., 2020. Biosens. Bioelectron. 171, 112686.
Gong, J., Dong, H., Xia, S.Q., Huang, Y.Z., Wang, D., Zhao, Y., Liu, W., Tu, S., Zhang, M., Wang, Q., Lu, F., 2020. MedRxiv. https://doi.org/10.1101/2020.02.25.20025643.
Huang, C., Wen, T., Shi, F.J., Zeng, X.Y., Jiao, Y.J., 2020. ACS Omega 5, 12550–12556.
Kailashiya, J., Singh, N., Singh, S.K., Agrawal, V., Dash, D., 2015. Biosens. Bioelectron. 65, 274–280.
Kucirka, L.M., Lauer, S.A., Laeyendecker, O., Boon, D., Lessler, J., 2020. Ann. Intern. Med. 173, 262–267.
Lan, L., Xu, D., Ye, G., Xia, C., Wang, S., Li, Y., Xu, H., 2020. J. Am. Med. Assoc. 323, 1502–1503.
Li, Q., Guan, X., Wu, P., Wang, X., Zhou, L., Tong, Y., Ren, R., Leung, K.S.M., Lau, E.H.Y., Wong, J.Y., Xing, X., Xiang, N., et al., 2020. N. Engl. J. Med. 382, 1199–1207.
Li, Z., Yi, Y., Luo, X., Xiong, N., Liu, Y., Li, S., Sun, R., Wang, Y., Hu, B., Chen, W., Zhang, Y., Wang, J., et al., 2020. J. Med. Virol. 92, 1518–1524.
Liv, L., 2021. Microchem. J. 168, 106445.
Oran, D.P., Topol, E.J., 2020. Ann. Intern. Med. 173, 362–367.
Park, M., Won, J., Choi, B.Y., Lee, C.J., 2020a. Exp. Mol. Med. 52, 963–977.
Park, S.W., Cornforth, D.M., Dushoff, J., Weitz, J.S., 2020b. Epidemics 31, 1–18.
Sanchez, S., Pumera, M., Fabregas, E., 2007. Biosens. Bioelectron. 23, 332–340.
Seo, G., Lee, G., Kim, M.J., Baek, S., Choi, M., Ku, K.B., Lee, C., Jun, S., Park, D., Kim, H. G., Kim, S., Lee, J., et al., 2020. ACS Nano 14, 5135–5142.
Torrente-Rodríguez, R.M., Lukas, H., Tu, J., Min, J., Yang, Y., Xu, C., Rossiter, H.B., Gao, W., 2020. Matter 3, 1–18.
Tran, Q.H., Nguyen, T.H.H., Mai, A.T., Nguyen, T.T., Vu, Q.K., Phan, T.N., 2012. Adv. Nat. Sci. Nanosci. Nanotechnol. 3, 015012.
Vadlamani, B.S., Uppal, T., Verma, S.C., Misra, M., 2020. Sensors 20, 5871.
Van Kasteren, P.B., van der Veer, B., van den Brink, S., Wijsman, L., de Jonge, J., van den Brandt, A., Molenkamp, R., Reusken, C.B.E.M., Meijer, A., 2020. J. Clin. Virol. 128, 104412.
Wang, H., Cai, H.H., Zhang, L., Cai, J., Yang, P.H., Chen, Z.W., 2013. Biosens. Bioelectron. 50, 167–173.
WHO, 2020a. Novel coronavirus (2019-nCoV) situation report - 1, 2020-11-05. https://www.who.int/docs/default-source/coronaviruse/situationreports/20200121-sitrep-1-2019-ncov.pdf?sfvrsn=20a99c10_4.
WHO, 2020b. Coronavirus disease 2019 (COVID-19): situation report - 52, 2020-11-05. https://www.who.int/docs/default-source/coronaviruse/situation-reports/20200312-sitrep-52-covid-19.pdf?sfvrsn=e2bfc9c0_4.
WHO, 2020c. COVID-19 – a global pandemic, what do we know about SARS-CoV-2 and COVID-19?, 2020-10-10. https://www.who.int/docs/default-source/coronaviruse/risk-comms-updates/update-28-covid-19-what-we-know-may-2020.pdf?sfvrsn=ed6e286c_2.
WHO, 2020d. Coronavirus disease (COVID-19) pandemic, 2021-04-09. https://www.who.int/emergencies/diseases/novel-coronavirus-2019?gclid=CjwKCAjw07qDBhBxEiwA6pPbHsBSqj6rxffYC6MEXGAC8a2cMutNVTEexOBFWPqL49glF6Qe6ASqwBoCnWMQAvD_BwE.
Yang, M., Chen, S., Huang, B., Zhong, J., Su, H., Chen, Y., Cao, Q., Ma, L., He, J., Li, X., Li, X., Zhou, J., et al., 2020. Eur. Urol. Focus 6, 1124–1129.
Zeng, L., Li, Y., Liu, J., Guo, L., Wang, Z., Xu, X., Song, S., Hao, C., Liu, L., Xin, M., Xu, C., 2020. Mater. Chem. Front. 4, 2000–2005.
Zhao, H., Liu, F., Xie, W., Zhou, T.C., OuYang, J., Jin, L., Li, H., Zhao, C.Y., Zhang, L., Wei, J., Zhang, Y., Li, C., 2021. Sensor. Actuator. B Chem. 327, 128899.
Zhu, J., Guo, J., Xu, Y., Chen, X., 2020. J. Infect. 81, E48–E50.